



Contents lists available at ScienceDirect

Science of the Total Environment

journal homepage: www.elsevier.com/locate/scitotenv

Comparison of five methodologies to apportion organic aerosol sources during a PM pollution event

D. Srivastava^{a,b,c}, K.R. Daellenbach^d, Y. Zhang^a, N. Bonnaire^e, B. Chazau^d, E. Perraudin^{b,c}, V. Gros^e, F. Lucarelli^f, E. Villenave^{b,c}, A.S.H. Prévôt^d, I. El Haddad^d, O. Favez^a, A. Albinet^{a,*}

^a Ineris, Parc Technologique Alata, BP 2, 60550 Verneuil-en-Halatte, France

^b CNRS, EPOC, UMR 5805 CNRS, 33405 Talence, France

^c Université de Bordeaux, EPOC, UMR 5805 CNRS, 33405 Talence, France

^d Paul Scherrer Institute (PSI), 5232 Villigen, Switzerland

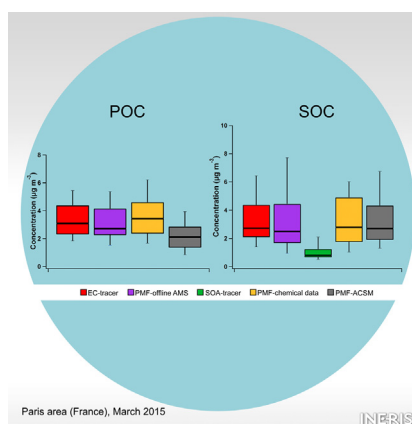
^e LSCE - UMR8212, CNRS-CEA-UVSQ, 91191 Gif-sur-Yvette, France

^f University of Florence, Dipartimento di Fisica Astronomia, 50019, Sesto Fiorentino, Italy

HIGHLIGHTS

- Comparison of 5 OA apportionment methodologies based on filter/on-line measurements
- Similar estimates from all approaches for total POA and SOA (except SOA-tracer)
- Discrepancies noticed between individual POA and directly comparable SOA estimates
- No approach able to identify the mechanisms/precursors from the highly oxidized SOA.
- A combination of different methodologies to apportion POA/SOA is recommended.

GRAPHICAL ABSTRACT



ARTICLE INFO

Article history:

Received 8 August 2020

Received in revised form 12 October 2020

Accepted 14 October 2020

Available online xxx

Editor: Pingqing Fu

Keywords:

Aerosols
EC-tracer
SOA-tracer
PMF
Offline AMS
ACSM

ABSTRACT

This study presents a comparison of five methodologies to apportion primary (POA) and secondary organic aerosol (SOA) sources from measurements performed in the Paris region (France) during a highly processed PM pollution event. POA fractions, estimated from EC-tracer method and positive matrix factorization (PMF) analyses, conducted on measurements from PM₁₀ filters, aerosol chemical speciation monitor (ACSM) and offline aerosol mass spectrometry (AMS), were all comparable ($2.2\text{--}3.7\ \mu\text{g m}^{-3}$) as primary organic carbon (POC). Associated relative uncertainties (measurement + model) on POC estimations ranged from 8 to 50%. The best apportionment of primary traffic OA was achieved using key markers (EC and 1-nitropyrene) in the chemical speciation-based PMF showing more pronounced rush-hour peaks and greater correlation with NO_x than other traffic related POC factors. All biomass burning-related factors were in good agreement, with a typical diel profile and a night-time increase linked to residential heating. If PMF applied to ACSM data showed good agreement with other PMF outputs corrected from dust-related factors (coarse PM), discrepancies were observed between individual POA factors (traffic, biomass burning) and directly comparable SOA factors and highly oxidized OA. Similar secondary organic carbon (SOC) concentrations ($3.3 \pm 0.1\ \mu\text{g m}^{-3}$) were obtained from all approaches, except the SOA-tracer method ($1.8\ \mu\text{g m}^{-3}$). Associated uncertainties ranged from 14 to 52% with larger uncertainties obtained for PMF-chemical data, EC- and SOA-tracer methods. This latter significantly underestimated total

* Correspondence to: A. Albinet, Ineris, 60550 Verneuil en Halatte, France.

E-mail addresses: deepchandra.srivastava@gmail.com (D. Srivastava), alexandre.albinet@ineris.fr, alexandre.albinet@gmail.com (A. Albinet).

SOA loadings, even including biomass burning SOA, due to missing SOA classes and precursors. None of the approaches was able to identify the formation mechanisms and/or precursors responsible for the highly oxidized SOA fraction associated with nitrate- and/or sulfate-rich aerosols (35% of OA). We recommend the use of a combination of different methodologies to apportion the POC/SOC concentrations/contributions to get the highest level of confidence in the estimates obtained.

© 2020 Elsevier B.V. All rights reserved.

1. Introduction

Airborne organic aerosols (OA) are commonly classified as primary (POA), i.e., directly emitted, or secondary (SOA), i.e., resulting from chemical (trans-) formation processes occurring in the atmosphere (Hallquist et al., 2009). POA and SOA have major impacts on human health, biogeochemical cycles and the Earth's climate (Heal et al., 2012; Boucher et al., 2013). However, determining their origin remains challenging due to the complexity and variability of the processes involved (Donahue et al., 2009). Most common methodologies applied to apportion POA and/or SOA include: elemental carbon-tracer (EC) approach (Grosjean, 1984; Turpin and Huntzicker, 1995; Gray et al., 1986), various statistical receptor models (e.g. chemical mass balance (CMB) and positive matrix factorization (PMF)) (Watson et al., 1990; Paatero, 1997; Paatero and Tapper, 1994), SOA-tracer method (Kleindienst et al., 2007) and radiocarbon (^{14}C) measurements (Szidat et al., 2009; Gelencsér et al., 2007). These methodologies have been successfully applied worldwide and, in general, good agreements have been reported when compared by twos directly (Song et al., 2006; Kim et al., 2004; Kleindienst et al., 2010; Pachon et al., 2010; Heo et al., 2013; Al-Naiema et al., 2018; Srivastava et al., 2018b; Bove et al., 2018; Bae et al., 2019; Antony Chen and Cao, 2018; Hettiyadura et al., 2018; Jiang et al., 2018; Keerthi et al., 2018; Matawle et al., 2018; Shi et al., 2018; Shirmohammadi et al., 2016; Lanzafame et al., 2020). However, large discrepancies have been also observed when apportioning the SOA fraction, depending on the methods compared, the period of the year considered or atmospheric conditions observed (Srivastava et al., 2018b). As an example, in a recent study conducted in the Paris region (France) by Lanzafame et al. (2020), a good agreement between total secondary organic carbon (SOC) estimations, evaluated by the SOA-tracer method and the filter-based PMF analysis, was observed over the year investigated, but substantial differences were noticed during a secondary PM (particulate matter) pollution event (where ammonium nitrate dominated). Similar observations have been reported by other authors during high pollution episodes or when high secondary contributions were observed (Srivastava et al., 2018b; Zhang et al., 2009; Hu et al., 2010; El Haddad et al., 2011; Feng et al., 2013).

Such high secondary pollution episodes are often observed in Western Europe during late winter–early spring (Petit et al., 2015; Dupont et al., 2016; Petit et al., 2017; Tarrasón et al., 2016; Hamer et al., 2017). PM pollution episodes are defined when the daily PM_{10} concentrations exceeded the European regulatory threshold of $50 \mu\text{g m}^{-3}$ for at least 3 consecutive days. Emissions from domestic heating, road transport and manure spreading along with anticyclonic atmospheric conditions result in the transport and/or accumulation of pollutants, as well as photochemical processes, within the boundary layer during such events (Waked et al., 2014; Petit et al., 2017; Dupont et al., 2016). Thus, such episodes are often dominated by a high proportion of secondary pollutants (especially ammonium nitrate and SOA) (Petit et al., 2017; Beekmann et al., 2015; Srivastava et al., 2018a; Srivastava et al., 2018c; Waked et al., 2014; Weber et al., 2019; Putaud et al., 2004; Putaud et al., 2010). Similar events have been observed in China in recent years; reduction in SO_2 emissions results in the shift of sulfate to nitrate dominated haze pollution events (Xie et al., 2020; Xu et al., 2019; Tian et al., 2019; Wang et al., 2020). During such events, organic matter (OM) is the second contributor to the PM mass concentrations observed

(Putaud et al., 2004) and, as meteorological and photooxidant conditions promote chemical processes, a significant fraction of OA is probably of secondary origin (Zhang et al., 2019; Huang et al., 2014; Petit et al., 2017; Srivastava et al., 2018a; Srivastava et al., 2019; Srivastava et al., 2018c; Tomaz et al., 2017). However, OA sources during these highly processed PM pollution episodes are still poorly addressed while it is critical in terms of air quality policy management. Subjectivity in the choice of the source apportionment method, final solutions and the assumptions applied, might have strong impacts on the results and conclusions obtained. Comparison of results obtained from different approaches to apportion POA/SOA fractions during such events would highlight discrepancies and uncertainties between each approach and further understanding of OA sources.

In this work, POA and SOA fractions have been resolved using various source apportionment methods, applied to different offline/online datasets collected from a short-term intensive campaign in the Paris area (France) during a springtime PM pollution event. PMF analyses have been conducted using extensive filter-based chemical speciation data, as well as OA mass spectra obtained from online aerosol chemical speciation monitor (ACSM) and offline filter-based aerosol mass spectrometry (AMS) measurements. EC-tracer and SOA-tracer methods have also been applied to the filter-based dataset. Overall, this study evaluates the consistency of outputs retrieved from these methodologies and explores their potential limitations when applied independently to each other in a highly processed environment. To the best of our knowledge, this work is one of the few source apportionment analyses applied to PM pollution episodes to characterize and/or investigate the existing difference between the approaches for OA sources.

2. Experimental

Details about the monitoring site, online measurements, sample collection, chemical speciation analytical procedures as well as backward trajectory analyses have already been reported in two previous articles (Srivastava et al., 2019; Srivastava et al., 2018a) and in the supporting material of the present one (SM). Only the essential information is presented in this section.

2.1. Monitoring site

Measurements were conducted at the ACTRIS-SIRTA observatory (Site Instrumental de Recherche par Télédétection Atmosphérique, 2.15°E ; 48.71°N ; 150 m; <http://sirta.ipsl.fr>), a well-established facility for the long-term monitoring of physical and chemical aerosol properties in the Paris area (France) (Zhang et al., 2019; Haeffelin et al., 2005). The site is located approximately 25 km southwest of Paris city center and is considered as representative of the background air quality of the Ile-de-France region with influence of the Paris plume under anticyclonic conditions. An intensive campaign was conducted on purpose during a PM pollution event (daily PM_{10} concentrations $>50 \mu\text{g m}^{-3}$ for several consecutive days) from 6 to 21 March 2015.

2.2. Online instrumentation

PM_{10} (TEOM 1405F, Thermo), NO_x (T200UP, Teledyne API), O_3 (T400, Teledyne API) and black carbon (BC) (aethalometer AE33,

Magee Scientific) concentrations were measured at 15, 1, 1 and 1-min time resolutions, respectively. In addition, meteorological parameters such as temperature, relative humidity (RH), wind direction, and wind speed were also measured at 1-min time resolution. The ACSM (Aerodyne Research) allowed for the measurement of major submicron (PM_{10}) non-refractory (NR) chemical species at about 30-min time resolution. Details on these measurements can be found elsewhere (Petit et al., 2017; Zhang et al., 2019). The ACSM dataset used in this work has already been reported previously (Srivastava et al., 2019).

2.3. Filter sample collection and analysis

A high-volume sampler (DA-80, Digitel; flow rate: $30 \text{ m}^3 \text{ h}^{-1}$) was used to collect PM_{10} samples (Tissu-quartz fibre filter, Pallflex, $\varnothing = 150 \text{ mm}$) every 4 h. A total number of 92 filter samples were collected and analyzed for an extended chemical speciation. Major ions (Cl^- , NO_3^- , SO_4^{2-} , NH_4^+ , Ca^{2+} , Na^+ , Mg^{2+} , K^+) (Guinot et al., 2007; CEN, 2017), EC and organic carbon (OC) (CEN, 2017; Cavalli et al., 2010), 7 elemental species (Ca, Ti, Mn, Fe, Ni, Cu, Pb), methanesulfonic acid (MSA), oxalate ($C_2O_4^{2-}$), 3 anhydrosugars (levoglucosan, mannosan and galactosan), 3 polyols/sugar alcohols (arabitol, sorbitol and mannitol) (Verlhac et al., 2013; Yttri et al., 2015), 9 polycyclic aromatic hydrocarbons (PAHs), 14 oxy-PAHs, 8 nitro-PAHs (Albinet et al., 2014; Albinet et al., 2013; Albinet et al., 2006; Tomaz et al., 2016) and 13 SOA markers (e.g., α -methylglyceric acid, pinic acid, and methyl-nitrocatechols) (Albinet et al., 2019; Srivastava et al., 2018c) were analyzed following the protocols already detailed previously. Offline AMS analysis focusing on the bulk composition of the organic aerosol was also performed on PM_{10} filter samples following the procedure developed previously (Daellenbach et al., 2016).

2.4. Source apportionment approaches

Each source apportionment methodology (EC-tracer, SOA-tracer and PMF analyses performed on the different datasets) is briefly discussed below. Details on the calculation of the overall uncertainties (measurement + model) linked to POC and SOC estimates using these approaches are presented in the SM. Limitations linked to these approaches are also briefly discussed in the SM and also explained elsewhere (Srivastava et al., 2018b). Note that for measurements, the uncertainties linked to the sampling were not considered. For filter-based methodologies, the uncertainty on the sampling volume collected would have been the same for all the methods and usually accounts for a minor part of the measurement uncertainty (Ringuet et al., 2012; Albinet et al., 2013; Albinet et al., 2014). In addition, as no denuder has been used for the PM_{10} filter samplings, we are aware that some sampling artifacts (positive, overestimation of the concentrations, or negative, underestimation, due to the sorption or desorption on/from the filter of semi-volatile species and/or due to the degradation/formation of chemical species by heterogeneous processes involving atmospheric oxidants) could induce additional measurement uncertainties, notably for the different organic species quantified here, but that are really difficult to evaluate (Albinet et al., 2010; Goriaux et al., 2006; Mader and Pankow, 2001; Turpin et al., 2000 and references therein). Similarly, uncertainties linked to the measurement artifacts with ACSM or off-line AMS due to the CO_2^+ / NO_3 effect (Pieber et al., 2016; Freney et al., 2019), were not considered in the overall uncertainty estimations.

2.4.1. EC-tracer method

The EC-tracer method has been widely used to estimate the partitioning of measured particulate OC into primary and secondary fractions (Grosjean, 1984; Turpin and Huntzicker, 1995; Castro et al., 1999; Chu, 2005; Saylor et al., 2006; Gray et al., 1986). Briefly, it takes advantage of primary OC and EC co-emissions to estimate SOC from the magnitude of OC-to-EC ratios measured in ambient air (Srivastava et al., 2018b). Here, a primary OC-to-EC ratio ($[OC/EC]_p$) of 2.9 was

estimated from the measurements during the periods of low photochemical activity. This $[OC/EC]_p$ value was used to calculate SOC concentrations (Fig. S1).

2.4.2. PMF-based approaches

Detailed information on PMF principle can be found elsewhere (Paatero and Tapper, 1994; Paatero, 1997). Briefly, this receptor model resolves factor profiles and contributions from a time series of observations using weighted least-squares fitting approach, where the weights are adjusted according to measurement uncertainties. The choice of the optimal solution is notably based on the minimization of the residuals obtained between modeled and observed input species concentrations.

The U.S. Environmental Protection Agency (US-EPA) PMF 5.0 toolkit has been used to perform the source apportionment on the PM_{10} filter chemical dataset (including inorganic species and metals, along with EC, OC and organic markers). As detailed in Srivastava et al. (2018a), OC concentrations obtained for each relevant factor were then used in this study (Figs. S2 and S3).

The information linked to OA source apportionment using the OA mass spectra from ACSM has been given by Srivastava et al. (2019) (Fig. S4). The offline-AMS PMF analyses details are provided in the SM (Figs. S5 to S11). For these analyses, OA mass spectra were treated using the Source Finder toolkit (SoFi) (Canonaco et al., 2013). OC concentrations related to the ACSM factors were further calculated applying OC-to-OA conversion factors specific to each source, i.e., 1.7 for biomass burning (Puxbaum et al., 2007), 1.2 for vehicular emissions (van Drooge and Grimalt, 2015) and 2.0 for secondary organics (Mohr et al., 2009). In the case of offline-AMS, OC-to-OA ratio was determined as explained by Canagaratna et al. (2015) and used to evaluate the OC concentrations of relevant OA factors.

Both US-EPA and SoFi toolkits use the multilinear engine (ME-2) algorithm, allowing the implementation of constraints on the factor chemical profiles and/or time series.

2.4.3. SOA-tracer method

The SOA-tracer method was developed to estimate the contribution of SOA fractions associated with individual gaseous precursors. SOC mass fractions are estimated using conversion factors to calculate SOC loadings from molecular marker concentrations (Kleindienst et al., 2007). A clear limitation of this methodology is related to the fact that only a limited number of organic markers can be accounted (Srivastava et al., 2018b).

SOC mass fractions (anthropogenic and biogenic) were modified according to a subset of markers analyzed following the procedure discussed previously (Rutter et al., 2014) (Tables S1 and S2). In addition, biomass burning SOA fraction was also estimated using the SOA-tracer method. Neglecting this SOA source might lead to significant underestimation of the total wintertime SOC concentrations in Europe due to relatively high contributions of residential wood burning during the cold season (Srivastava et al., 2018b; Petit et al., 2014; Ciarelli et al., 2017; Puxbaum et al., 2007; Daellenbach et al., 2017; Srivastava et al., 2019; Languille et al., 2020). Details on the estimation of biomass burning SOA fraction can be found elsewhere (Lanzafame et al., 2020).

3. Results and discussion

3.1. Overview of the PM pollution event and chemical composition

An overview of the PM chemical composition during the studied period is given in Fig. 1. The daily PM_{10} concentrations were in the range of $12\text{--}130 \mu\text{g m}^{-3}$, with an average of $49 \mu\text{g m}^{-3}$. A large predominance of secondary inorganic species, especially ammonium nitrate, was observed during the pollution episode as expected highlighting the significance of secondary processes (Petit et al., 2017). OM concentrations ranged from 2 to $25 \mu\text{g m}^{-3}$, with an average value of about $12 \mu\text{g m}^{-3}$. Slight differences can be observed between the measured

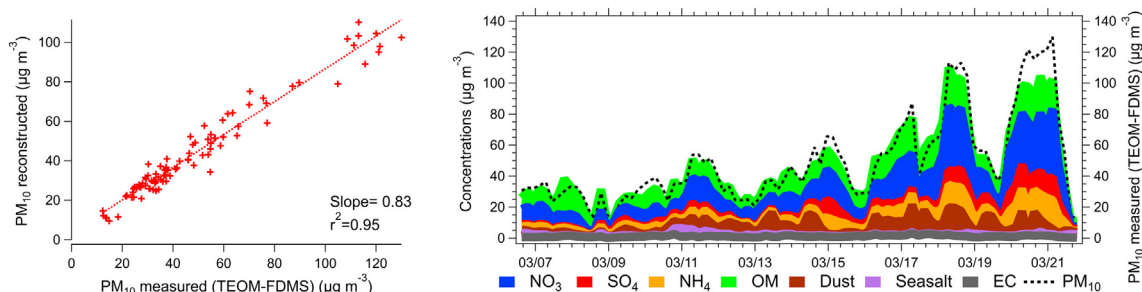


Fig. 1. Left: Comparison of the reconstructed PM₁₀ mass from chemical characterization and the PM₁₀ measured using TEOM-FDMS. Right: Relative contribution of the chemical species to PM₁₀ mass and temporal variations of the measured PM₁₀, PM₁ (NR-PM₁ + BC) at Paris-SIRTA, France (March 2015). Sea salt and dust were calculated applying the procedure explained by Bressi et al. (2014).

and the reconstructed PM₁₀ mass concentrations (slope of 0.83) due to the PM water content and/or some sampling artifacts together with the measurement uncertainties.

3.2. Number of distinguished POA and SOA classes

The identification of each of these factors is summarized in Table 1 and their contributions to total OC in PM₁₀ is shown in Fig. 2. As defined, the EC-tracer method resulted in the estimation of 1 primary and 1 secondary factor. The SOA-tracer method allowed for the quantification of 5 different SOA fractions corresponding to the 5 categories of SOA markers used. PMF analysis conducted on the chemical dataset (PMF-chemical data) led to the discrimination of 10 different OA factors, while analyses on the offline AMS and ACSM datasets (PMF-offline AMS and PMF-ACSM) allowed the identification of 6 and 4 OA factors, respectively. Note that, as ACSM measurements consider only the PM₁, the difference between OC in PM₁₀ (from filter measurements) and in PM₁ was affected by coarse OC (Fig. 2).

Combustion-related factors highly influenced by primary organic molecular markers (for PMF-chemical data) or by hydrocarbon mass fragments (for PMF-offline AMS and PMF-ACSM) were attributed to the POA fraction. The factors mainly influenced by secondary markers or oxygenated mass fragments were ascribed to the SOA fraction. Dust-related OA factors (retrieved from PMF-chemical data as well as PMF-offline AMS) could be linked to both primary and secondary aerosols due to soil abrasion, resuspension and/or coagulation processes and to condensation of semi-volatile organic species onto mineral dust particles. The dust factor identified by PMF-chemical data contained a significant amount of EC (Fig. S2), along with metals (mainly crustal) and cations (Ti, Ca²⁺, Mg²⁺, Cu and Mn), with negligible amount of secondary species present in the factor profile. This supports the hypothesis of considering this factor to be primary. The SCOA (sulfur-containing OA)

factor identified by PMF-offline AMS characterized based on the presence of sulfur containing fragments (CH₃SO₂⁺) in the chemical profile, has been found to be mainly coarse and originate from primary emissions based on previous studies (Vlachou et al., 2018; Daellenbach et al., 2017; Bozzetti et al., 2016). This was also supported as it showed good correlations with crustal metals and therefore this “dust” factor has been attributed to the POA fraction.

Such a disparity in the number of identified factors impeded their direct comparison. However, the comparison of POA and SOA fractions apportioned can be discussed as follows.

3.3. Comparison of the POA factors

Fig. 3 shows the primary OC (POC) concentrations obtained from the different methodologies used for POA apportionment. On average, a good agreement between the outputs from EC-tracer method, PMF-chemical data, and PMF-offline AMS was observed (Fig. 3b). Averaged PM₁₀ POC concentrations obtained from these three methodologies ranged between 3.2 and 3.7 μg m⁻³ representing ~50% of the total PM₁₀ OC. Time series were rather similar (datasets normally distributed, paired *t*-test; *p*-values > 0.05) except between PMF-chemical data and PMF-offline AMS, as shown in Table S6a and Fig. 3a. However, significant disagreements can be observed during certain days (e.g. 10th, 16th, and 19th March) when the PMF-chemical data and EC-tracer showed high concentrations while both other approaches showed minimum levels. As discussed below, this is mainly due to the retrieval of the traffic-related POC source by the AMS/ACSM based approaches especially during morning rush hours (Figs. 4 and 5). The highest correlation (*r*² = 0.64, *n* = 92, *p* < 0.05) was observed between PMF-chemical data and EC-tracer method (Table S7a). The overall absolute uncertainties in the POC estimates were in the same range for all methods (about 0.5–1.8 μg m⁻³) strengthening the good agreement between

Table 1
List of POA and SOA factors retrieved from each source apportionment methodology.

Method	Size fraction	Temporal resolution	Primary factors		Secondary factors	
			Number	Labelling	Number	Labelling
EC-tracer method	PM ₁₀	4 h	1	POA	1	SOA
SOA-tracer method	PM ₁₀	4 h	Not applicable		5	Isoprene SOA, α-Pinene SOA, Toluene SOA, Naphthalene SOA, Biomass burning (phenolic compounds) SOA
PMF-chemical data	PM ₁₀	4 h	3	Primary traffic emissions; Biomass burning; Dust	7	Biogenic SOA-1; Biogenic SOA-2 Anthropogenic SOA-1; Anthropogenic SOA-2; Anthropogenic SOA-3; Mixed secondary; Nitrate-rich
PMF-offline AMS	PM ₁₀	4 h	4	Traffic POA (hydrocarbon-like OA (HOA), tailpipe/engine); Cooking POA (COA); Biomass burning POA (BBOA); Sulfur-containing OA (SCOA, coarse POA)	2	Oxidized oxygenated OA 1 and 2 (OOA1; OOA2)
PMF-ACSM	PM ₁	0.5 h	2	Traffic POA (HOA, tailpipe/engine); Biomass burning POA (BBOA)	2	More oxidized oxygenated OA (MO-OOA); Low oxidized oxygenated OA (LO-OOA)

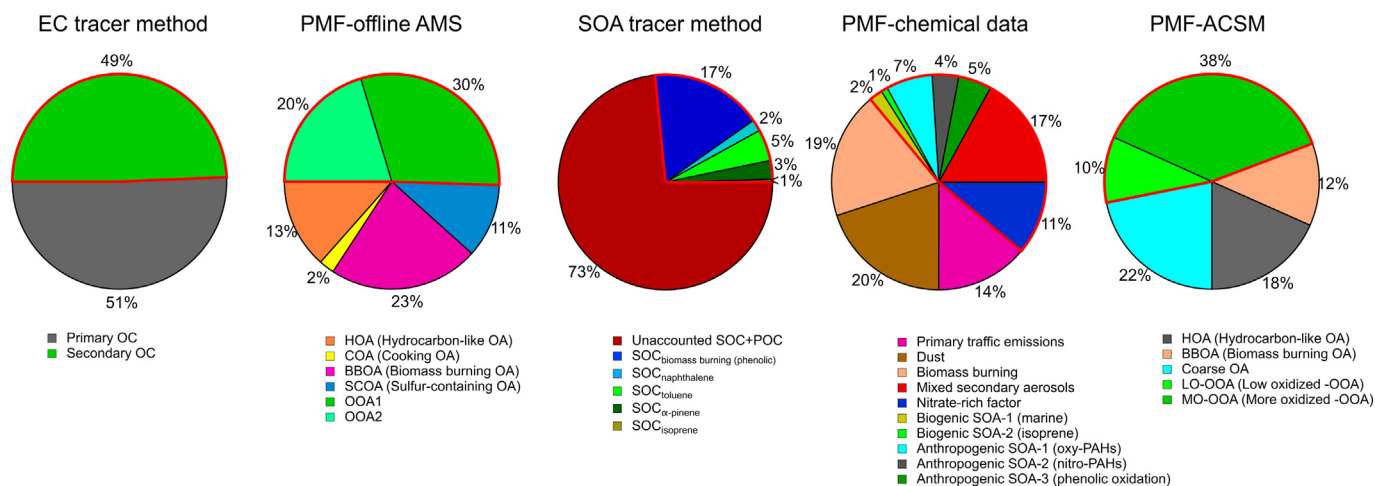


Fig. 2. Contribution of primary and secondary factors to the total PM₁₀ OC mass (in the case of PMF-ACSM PM₁), retrieved from the different source apportionment approaches. Red border represents the total secondary fractions. Note, colours used for the PMF-chemical and PMF-ACSM pie-charts are the same as already published (Srivastava et al., 2018a; Srivastava et al., 2019). (For interpretation of the references to colour in this figure legend, the reader is referred to the web version of this article.)

the different methodologies used. EC-tracer and PMF off-line AMS showed low relative overall uncertainties (32% vs. 15%, respectively). However, larger uncertainties (50% vs 15% as relative uncertainties) have been obtained for the PMF-chemical data approach (Fig. 3b). It has already been shown that measurement uncertainties, linked to the chemical analysis of the PMF input species (Tables S4 and S5), played a major contribution to the overall uncertainty (Pachon et al., 2010). Here, we tried to consider all the possible sources of uncertainties from the chemical analysis procedures,

notably applying a GUM (Guide to the Expression of Uncertainty in Measurement) approach for most of the organic markers (González et al., 2018; White, 2008). In the end, about 90% of the total estimated uncertainty was associated to the measurement uncertainty and the PMF model uncertainty, estimated following the recommendations of Brown et al. (2015), accounted only for 10%. This highlights that the evaluation of analytical uncertainties must be considered very cautiously given that the input species in the PMF model are weighted by uncertainties.

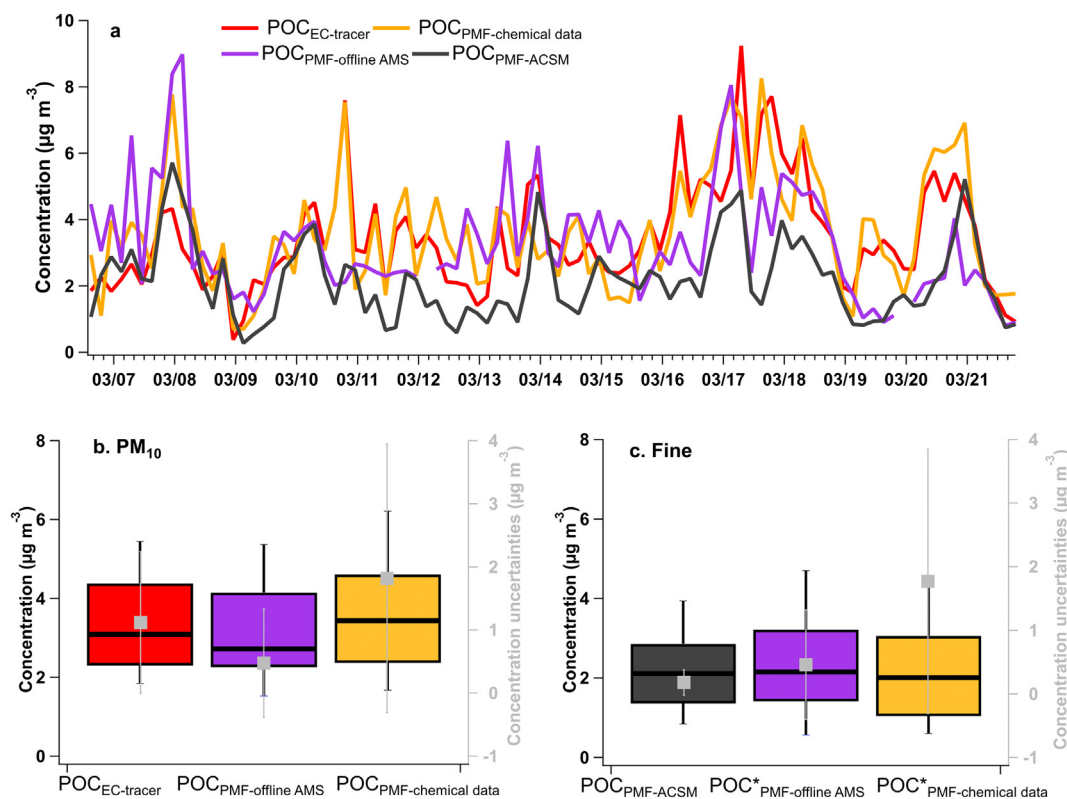


Fig. 3. Comparison of total POC concentrations obtained from the different source apportionment methodologies: a: Time series. b: Box-plots show the minimum, first quartile, median, third quartile and maximum values for PM₁₀ OA. c: Box-plots for the fine OA fraction with POC*_{PMF-chemical data}: PMF-chemical data without dust (primary traffic emissions + biomass burning); POC*_{PMF-offline AMS}: PMF-offline AMS without SOC (= hydrocarbon-like OC (HOC) + biomass burning OC (BBOC) + cooking OC (COC)); POC_{PMF-ACSM} = HOC + BBOC. Gray square symbols: POC median overall uncertainties $\pm 2\sigma$.

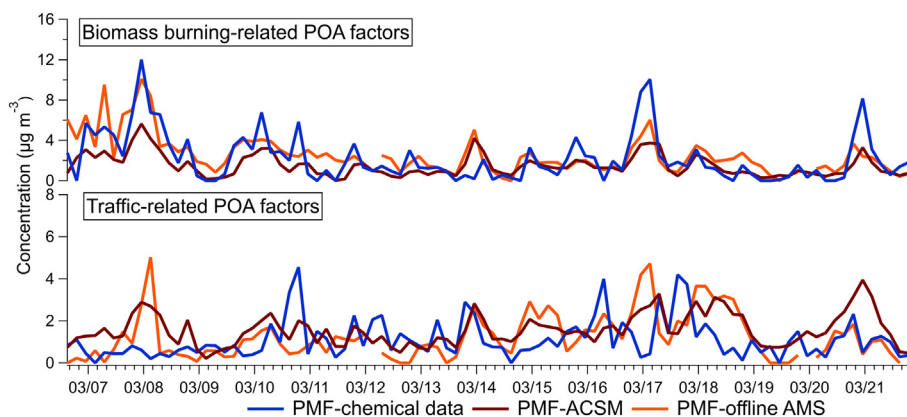


Fig. 4. Time series of biomass burning- (top panel) and traffic-related (bottom panel) POC factors obtained from the three PMF approaches.

POC concentrations estimated from the PMF-ACSM analysis were significantly lower (datasets normally distributed, paired t -test; p -value < 0.05) than the three other ones (about $2.2 \mu\text{g m}^{-3}$) (Fig. 3a and Table S6a). This result is mainly related to the difference in the sampling size cut-off between ACSM and filter samplings (PM_{10} for ACSM $< \text{PM}_{10}$ for filter samples). The time series of POC fraction from the EC-tracer method correlated well with that from PMF-chemical data, while the POC variations of PMF-offline AMS were much similar with those of PMF-ACSM. These results are likely due to the similarity in chemical composition of the different datasets as the EC-tracer method and PMF-chemical data are based on filter measurements, and on the other side, offline AMS and ACSM both measured the NR-PM species including organics, sulfate, nitrate, ammonium and chloride. As presented in Figs. 2 and S12, the average contribution of the submicron fraction to total OA concentrations was about 77%. The remaining 23% were associated to the coarse OA fraction and possibly attributed to the dust/SCOA factors (20% and 11%, respectively) identified using PMF-chemical data and PMF-offline AMS methodologies.

Considering only the fine OA fraction, total POC concentrations from PMF-ACSM showed a good agreement with both other PMF approaches namely, PMF-offline AMS and PMF-chemical data (Table S7b). However, a significant difference (datasets normally distributed, paired t -test; p -values < 0.05) was found between PMF-ACSM and PMF-offline AMS (so without SCOA) (Table S6a). On average for the whole period of the study, total fine POC concentrations ranged from $2.2 \mu\text{g m}^{-3}$ (PMF-ACSM) to $2.5 \mu\text{g m}^{-3}$ (PMF-offline AMS). As observed for the PM_{10} POC, overall uncertainties estimated for the PMF-chemical data

method (78%) were much higher than those obtained for both other PMF approaches based on aerosol mass spectrometry measurements (8–19%). Again, the consideration of all the possible sources of uncertainties of measurement by the GUM approach, increased the final uncertainty budget of the PMF-chemical data method. PMF-ACSM and PMF-offline AMS uncertainties were similar though the variability was higher for the PMF-offline AMS analysis. Recovery of OA factors in the offline-AMS analysis which is based on water soluble extraction can be considered responsible for this discrepancy as the hydrophobic nature of the components (e.g., HOA and COA) may lead to such kind of variation. The choice of the chemical profiles used could also have an impact on the overall uncertainty even if it was supposed to be low, as attempt has been made to choose very specific source specific chemical tracers, based on the literature.

Such a consistency in the fine OA fraction allowed to further compare individual primary PMF factors related to the main combustion sources: biomass burning- and traffic-related OA (Fig. 4). A good agreement was observed between all the identified biomass burning-related factors, with r^2 ranging from 0.48 to 0.61 (Table S8). Similar diel profiles were also obtained from the three PMF approaches, with a significant nighttime increase linked to residential heating activities (Fig. 5). As shown in Figs. 4 and S13, biomass burning-related factor concentration levels (0.67 – $1.19 \mu\text{g m}^{-3}$) were roughly equivalent throughout the campaign except for a few data points with slightly lower BBOA concentration levels for PMF-ACSM, notably at the beginning of the campaign, inducing a slight underestimation of BBOC by this method. Thus, a possible influence of the super-micrometer ($>1 \mu\text{m}$) biomass burning-related aerosols cannot be totally ruled-out. It may also be hypothesized

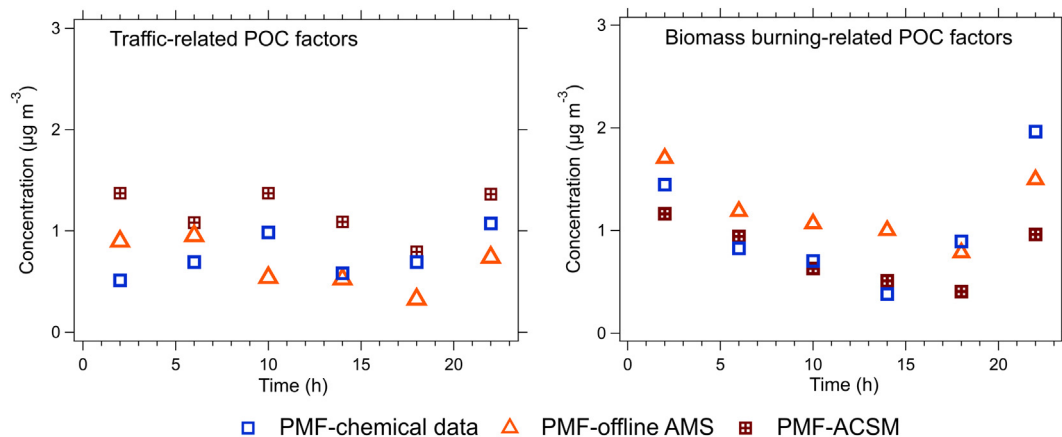


Fig. 5. Diel profiles of median values obtained for the traffic- and biomass burning-related OC factors using the different source apportionment methodologies (local time).

that biomass burning OA (ACSM) may be partly included in other factors than BBOA, such as HOA as already shown by some previous ACSM-based studies (Petit et al., 2014; Srivastava et al., 2019; Zhang et al., 2019). This was also supported by significant correlation ($r^2 = 0.45$, $n = 92$, $p < 0.05$) observed between BBOA and HOA factors from the PMF-ACSM analysis (Fig. S14).

Consequently, PMF-ACSM traffic related factor frequently showed slightly higher concentrations during biomass burning predominant periods (Figs. 4 and S13). It should also be noted that, on the diel cycle, the morning and evening rush-hours are more pronounced for the PMF-chemical data traffic factor than for the PMF-ACSM and PMF-offline AMS HOA factors (Fig. 5). In addition, traffic factor from PMF-chemical data is clearly better correlated with NO_x and BC_{ff} than the other traffic related POA factors (Fig. S15). These results suggested that the PMF-chemical data analysis could more accurately describe primary traffic-related OA, which might be related due to the use of key species, such as EC and 1-nitropyrene, in the input chemical data matrix (Srivastava et al., 2019; Srivastava et al., 2018c; Srivastava et al., 2018a; Lanzafame et al., 2020). As mentioned before, the disagreements observed at certain days (e.g. 10th, 16th March) are probably related to the better resolution of the traffic-related POC factor using PMF-chemical data approach. Nevertheless, the relatively good agreement between averaged traffic-related POC concentrations (i.e., about $0.9 \mu\text{g m}^{-3}$ for both PMF-chemical data and PMF-offline AMS, $1.1 \mu\text{g m}^{-3}$ for PMF-ACSM) validates the assumption of the predominant vehicular exhaust origin for HOC factors (Lanz et al., 2007; Xu et al., 2014; Ulbrich et al., 2009; Zhang et al., 2007). This suggests that HOA could be a proxy for traffic emissions but less well resolved than using proper markers. For both POA factors, biomass burning and traffic-related, estimated overall uncertainties were in a similar range ($0.1\text{--}2.5 \mu\text{g m}^{-3}$) strengthening the good agreement between the different methodologies for the estimation of these individual POC factors. Significantly higher uncertainty values were still observed for the PMF-chemical data (228% and 297% for traffic-related POA and for BBOA, respectively) (Fig. S13) suggesting again the significant influence of the measurement uncertainties especially considering all the potential sources of analytical uncertainties in that case. Large differences were also noticed in the relative overall uncertainties for both POA factors estimated using PMF-offline AMS and PMF-ACSM approaches (55% vs. 9% and 52% vs. 22% for HOA and BBOA, respectively) and probably linked to the measurement approaches (off-line vs. on-line measurements).

Finally, for the primary fraction, time series of the PMF-chemical data dust factor and the PMF-offline AMS SCOA factor showed a good agreement for few peaks (Fig. S16). This result suggested that SCOA is probably related in part to primary dust aerosols, in the coarse mode, as suggested previously (Vlachou et al., 2018; Daellenbach et al., 2017) but additional investigations are required to clearly identify the exact origin of that factor.

3.4. Comparison of the SOA factors

Total SOC concentrations showed a good agreement between all the source apportionment methodologies, except for the SOA-tracer method (Fig. 6 and Table S9). This observation was also confirmed as no statistical difference (datasets normally distributed, paired t -test; p -values > 0.05) was noticed between the different approaches (Table S6b).

Average SOC concentration values ($3.3 \pm 0.1 \mu\text{g m}^{-3}$) were similar for the EC-tracer method, PMF-chemical data, PMF-offline AMS and PMF-ACSM (Fig. 6b). Lower concentrations were derived from the SOA-tracer method (average value of about $1.8 \mu\text{g m}^{-3}$), especially for the second half of the campaign. $\text{SOC}_{\text{SOA-tracer}}$ concentrations obtained here only accounted for SOA formed from the oxidation of isoprene, α -pinene, naphthalene, toluene and phenolic compounds (see Section S2 in the SM). Due to the lack of information on other possible SOA hydrocarbon precursors, such as mono- and poly-aromatic compounds, long-chain alkanes and/or alkenes (Srivastava et al., 2018b; Zhao et al., 2014; Tkacik et al., 2012; Lim and Ziemann, 2005), the present SOA-tracer method analysis missed significant additional SOA classes. In addition, relatively high organonitrate and/or organosulfate loadings (Riva et al., 2015; Surratt et al., 2006; Tomaz et al., 2017) could be expected between the 15th and the 21st of March, a period when PM_{10} concentrations were highly dominated by water-soluble inorganic species (Fig. 1) (Srivastava et al., 2018a). However, it should be noted that total SOC concentrations estimated by the SOA-tracer method matched rather well with the outputs from other approaches during the first half of the campaign (before 14th March, Fig. 6a). This suggests relatively fair estimates of SOA-tracer individual factors considered in the present study and especially for biomass burning linked to the oxidation of phenolic compounds. This is further supported by the comparison between SOA-tracer method and PMF-chemical data outputs calculated over the yearlong (2015) measurement for the same site and showing a good agreement, especially for anthropogenic SOA (Lanzafame et al., 2020). Here, during this PM pollution event, the 3 PMF approaches especially PMF-ACSM and PMF-off-line AMS, were not able to capture the large biomass burning SOC peak observed with the EC- and SOA tracer methods at the beginning of the campaign (08th March) and was considered as POC (or at least in part as for PMF-chemical data). Note this SOC peak showed the same temporal variation as methyl-nitrocatechols, secondary photo-oxidation products of phenolic compounds (i.e., cresols), known to account for major SOA precursors emitted by biomass burning (Iinuma et al., 2010), confirming the actual secondary origin of OC at the beginning of the sampling campaign (Fig. S17).

The absolute uncertainties evaluated for SOC estimates seemed comparable with slightly higher values observed for the EC-tracer and PMF-chemical data methodologies (Fig. 6b) ($0.5\text{--}1.7 \mu\text{g m}^{-3}$). Considering the overall uncertainties obtained, average SOC estimations

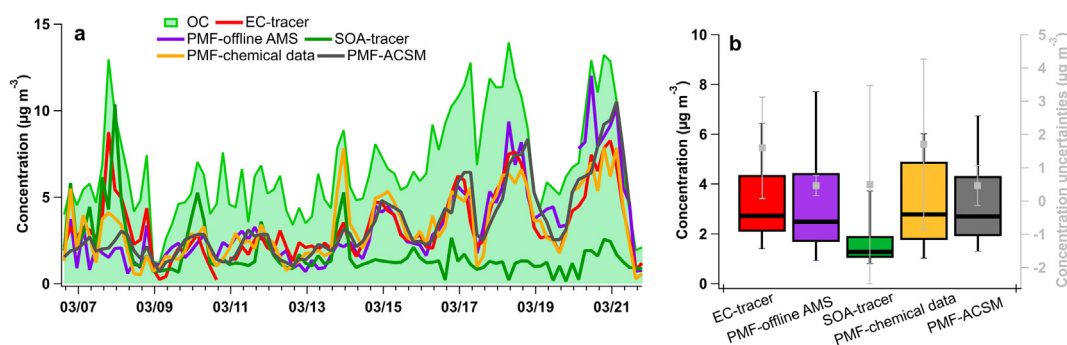


Fig. 6. Comparison of total SOC concentrations obtained from the different methodologies. a: Time series. b: Box-plots showing the minimum, first quartile, median, third quartile and maximum values. Gray square: error median $\pm 2\sigma$.

obtained with all the apportionment methodologies (except SOA-tracer method) used were in very good agreement. The higher uncertainties for the PMF-chemical data (52%) might be linked to the analytical uncertainties of the input species as discussed above (GUM approach for instance). However, the contribution of model uncertainty has increased here by 10% to the overall uncertainty. EC tracer method uncertainty was also high (48%) and mostly related to the primary [OC/EC] ratio evaluation during the cold period, as already reported as a major source of error in the estimation of secondary fraction using this SOC apportionment method (Srivastava et al., 2018b). These observations are consistent with previous results (Srivastava et al., 2018b; Pachon et al., 2010). PMF offline AMS and PMF-ACSM showed lower relative overall uncertainties of about 14%. Finally, the lower SOC estimations from the SOA-tracer method were also accompanied by comparable relative uncertainties to the other methods (about 27%).

Regarding the individual factors from all approaches, secondary biomass burning contribution resolved using the SOA tracer method and filter-based PMF analysis showed a very good agreement (Fig. S18). Both also showed a reasonable association with primary biomass burning factors resolved based on the mass spectrometry measurements (PMF-offline AMS and PMF-ACSM), indicating that these primary factors may contain some aged aerosols ($r^2 = 0.44\text{--}0.55$, $n = 92$, $p < 0.05$). SOC from the naphthalene oxidation obtained using the SOA tracer method agreed reasonably well with mixed secondary aerosols obtained by PMF-chemical data analysis ($r^2 = 0.55$, $n = 92$, $p < 0.05$).

In addition, highly oxidized OA factors (namely oxidized oxygenated OA (OOA1) and more oxidized oxygenated OA (MO-OOA)), from PMF-

offline AMS and PMF-ACSM analyses, respectively) and, marine biogenic SOA and mixed secondary aerosols obtained by PMF-chemical data analysis showed satisfactory correlations (Fig. 7) highlighting the similar origin of the given SOA factors. SOA derived from isoprene, α -pinene and toluene oxidation based on PMF-chemical data and SOA tracer method did not show any direct association with any of the secondary factors, probably due to their low contribution. Nevertheless, LO-OOA (from PMF-ACSM analysis) showed a substantial correlation with primary factors i.e., biomass burning and traffic emissions ($r^2 = 0.3\text{--}0.5$, $n = 92$, $p < 0.05$), suggesting the influence of anthropogenic emissions.

High concentrations of both highly oxidized OOA factors (OOA1, MO-OOA), marine biogenic SOA + mixed secondary aerosols and SOA from naphthalene oxidation were notably observed during the second half of the campaign (Fig. 8). Along with the significant inorganic loadings (Fig. 1), a probable predominant long-range transport influence might be expected during this period as reported before (Petit et al., 2017; Srivastava et al., 2018a). A comparable OOA factor has also been reported in winter in other European locations with similar characteristics namely, significant correlation with long range transported secondary inorganic species (Daellenbach et al., 2017; Lanz et al., 2007).

Both highly oxidized OOA factors may include a part of marine aerosols/traces of combustion aerosols (Srivastava et al., 2018a). This was supported as highly oxidized factors showed a good correlation with anthropogenic markers such as phthalic acid and succinic acid ($r^2 = 0.40\text{--}0.50$, $n = 92$, $p < 0.05$). However, no correlation was observed with sodium/chloride as expected for being considered as an influence of marine origin. Both OOA factors also captured a significant m/z 45

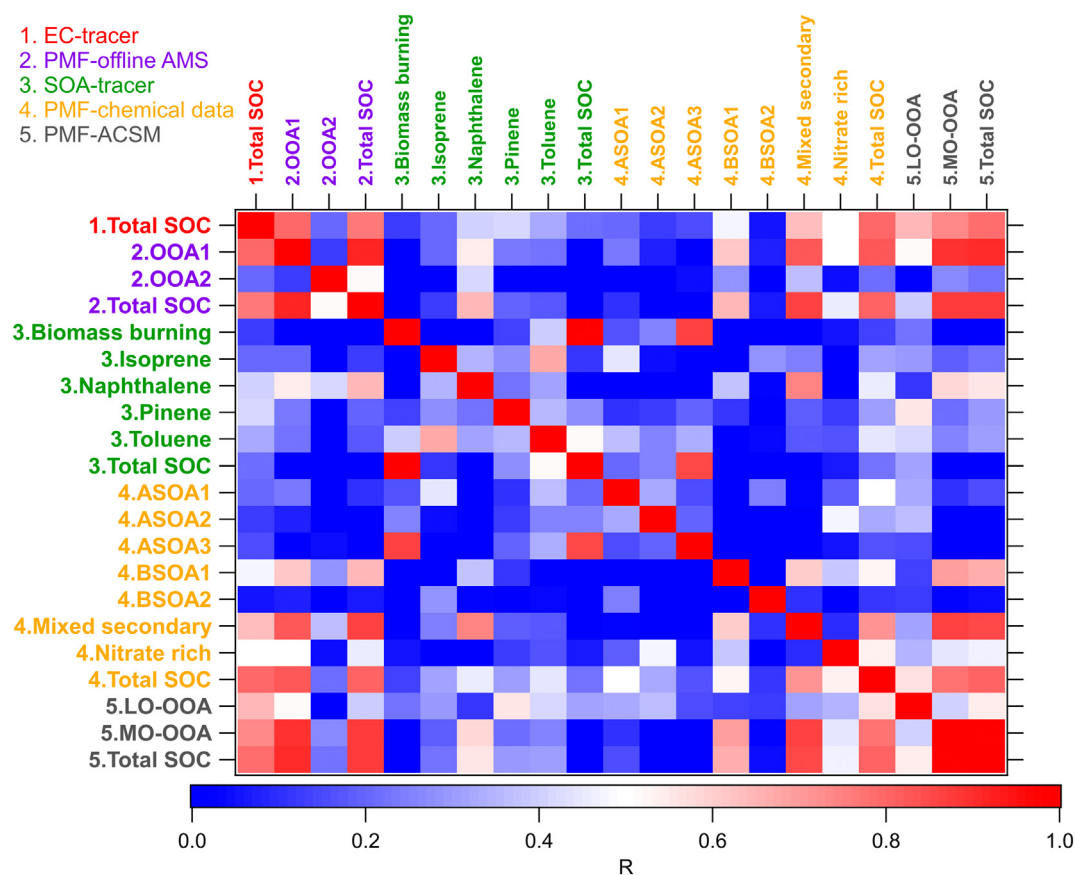


Fig. 7. Correlation matrix within individual OA factors resolved using all approaches. 1. EC-tracer method: 1. Total SOC; 2. PMF-offline AMS: 2. OOA1, 2. OOA2 and 2. Total SOC; 3. SOA-tracer: 3. Biomass burning (SOC biomass burning), 3. Isoprene (SOC isoprene), 3. Naphthalene (SOC naphthalene), 3. Toluene (SOC toluene) and 3. Total SOC; 4. PMF-chemical data: 4. BSOA-1 (Biogenic SOA (marine)), 4. BSOA-2 (Biogenic SOA (isoprene)), 4. ASOA-1 (Anthropogenic SOA (oxy-PAHs)), 4. ASOA-2 (Anthropogenic SOA (nitro-PAHs)), 4. ASOA-3 (Anthropogenic SOA (phenolic oxidation)), 4. Mixed secondary, 4Nitrate-rich and 4. Total SOC; 5. PMF-ACSM: 5. MO-OOA, 5. LO-OOA and 5. Total SOC.

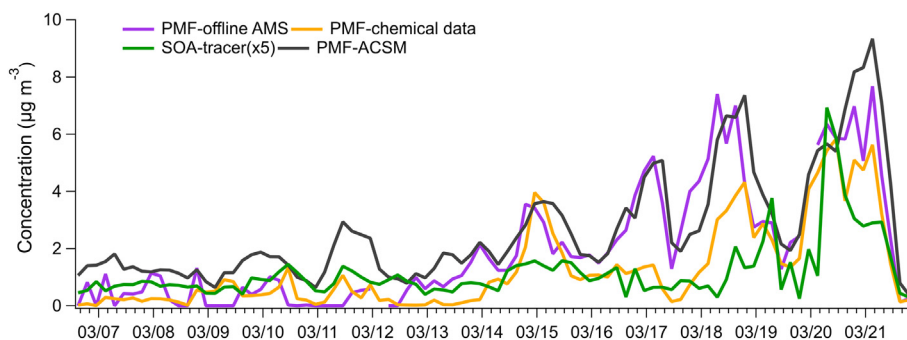


Fig. 8. Comparison of temporal variation of highly oxidized OA factors obtained from PMF-offline AMS (OOC1) and PMF-ACSM (MO-OOC), the sum of the mixed secondary aerosol and marine biogenic SOA factors obtained from PMF-chemical data and SOA-naphthalene from SOA-tracer method.

signal, a fragment observed from dicarboxylic acid, supporting the role of highly processed aerosols in ambient air, and has already observed in several studies (Zhang et al., 2005a; Zhang et al., 2005b; Jimenez et al., 2003; Bahreini et al., 2003). Mixed secondary aerosol factor, in the PMF-chemical data analysis, contained also ultimate oxidation by-products like oxalate which is not specific of any precursors or sources, confirming (Srivastava et al., 2018a) the aforementioned hypothesis. This highlighted that a significant amount of SOA could be linked to the aging of the air masses during long range transport, making it challenging to investigate its origins. Finally, none of the used approaches was able to fully identify the specific formation processes and/or the semi-volatile organic precursors responsible for this highly oxidized SOA fraction (accounting for about 35% of total OA in PM_{10} , ($r^2 > 0.80$, $n = 92$, $p < 0.05$)). Even combining off-line and on-line data set as reported before, a clear identification of the SOA sources/processes occurring during the last period of the campaign was not possible to achieve (Srivastava et al., 2019). Further studies are needed to investigate the secondary processes associated with nitrate- and/or sulfate-rich aerosols during such highly processed PM pollution events.

4. Conclusions

A comparison of five methodologies to apportion POA and SOA sources, during a PM pollution event in Northern Europe, has been performed.

POA fractions (average POC = $2.2\text{--}3.7 \mu\text{g m}^{-3}$) were well resolved using all approaches. Only lower POC concentrations were estimated by the PMF-ACSM analysis due to the difference in the sampling size cut-off (PM_1 vs PM_{10} for filter-based methods). PMF-chemical data POC estimates were associated with higher relative overall uncertainties (50% vs. 8%) due to the consideration of all the potential sources of errors in the sample chemical analyses.

Approximately half of the OA fraction was secondary (average concentrations = $3.3 \pm 0.1 \mu\text{g m}^{-3}$). However, the estimation of this fraction remains questionable during highly PM processed pollution events. The SOA-tracer method was not able to capture signals from other precursors dominant during the studied period and significantly underestimated SOC ($1.8 \mu\text{g m}^{-3}$). PMF-chemical data presented a good comparison with all other considered approaches and provided valuable information on the SOA contributions from different precursors. Similarly, SOC estimates from PMF-offline AMS and ACSM analysis were comparable, although they did not provide further insight on precursors and/or sources of highly oxidized fractions. The uncertainties of SOC estimates were broadly comparable in absolute value for all methods, but they were higher as relative values (14% vs. 52%) for the EC tracer, PMF-chemical data and SOA-tracer methods.

These results showed that more comprehensive studies focusing on the identification of new SOA tracers from known/unknown class of precursors are needed to fully understand the origins of SOA fractions.

Such studies would aid in bridging the gap between SOA contributions from models and measurements and explicitly improve our knowledge on SOA contribution in a highly oxidative environment. In addition, as recommended previously (Srivastava et al., 2018b), this study demonstrated that to get the highest level of confidence, it is recommended to use a combination of different methodologies, at least more than one, to apportion the POC/SOC concentrations/contributions. Such combination, especially if low and high time resolution measurements are used, could also enhance the understanding of the subtle differences in OA content.

Finally, the use of advanced instruments in near future such as TAG-AMS (thermal desorption aerosol gas chromatograph-AMS) (Williams et al., 2014), soft ionization methods like extractive electrospray (EESI) (Qi et al., 2020; Lopez-Hilfiker et al., 2019; Qi et al., 2019; Stefanelli et al., 2019), or aerosol inlets associated to PTR-MS (proton-transfer reaction-MS) or CIMS (chemical ionization MS) such as FIGAREO (filter inlet for gases and aerosols) (Lopez-Hilfiker et al., 2014), CHARON (chemical analysis of aerosol online) or thermo-desorption (TD) systems (Holzinger et al., 2010; Gkatzelis et al., 2017; Eichler et al., 2015), may provide more in-depth insight into the precursors and SOA formation processes involved during such highly processed PM pollution events.

CRedit authorship contribution statement

D. Srivastava: Conceptualization, Formal analysis, Data curation, Writing - original draft. **K.R. Daellenbach:** Formal analysis, Data curation. **Y. Zhang:** Formal analysis. **N. Bonnaire:** Formal analysis. **B. Chazeau:** Formal analysis. **E. Perraudin:** Supervision. **V. Gros:** Supervision. **F. Lucarelli:** Formal analysis. **E. Villenave:** Supervision. **A.S.H. Prévôt:** Formal analysis. **I. El Haddad:** Formal analysis. **O. Favez:** Conceptualization, Methodology, Supervision, Data curation. **A. Albinet:** Conceptualization, Methodology, Supervision, Data curation, Writing - original draft.

Declaration of competing interest

The authors declare that they have no known competing financial interests or personal relationships that could have appeared to influence the work reported in this paper.

Acknowledgements

This work has notably been supported by the French Ministry of Environment as part of the activities of the National reference laboratory for air quality monitoring (LCSQA). Aerosol in situ measurements have been performed as part of the H2020 ACTRIS-2 project and partly funded by the ACTRIS-Fr/CLAP initiative at the national level. This work is also the part of the COLOSSAL European COST Action CA16109. The

